ELSEVIER

Chemical Engineering Journal 132 (2007) 279–287

Chemical Engineering Journal

www.elsevier.com/locate/cej

Adsorption of phenol from aqueous solutions using mesoporous carbon prepared by two-stage process

L. John Kennedy [a], J. Judith Vijaya [b], K. Kayalvizhi [a], G. Sekaran [a,*]

[a] *Department of Environmental Technology, Central Leather Research Institute, Adyar, Chennai, Tamil Nadu, India*
[b] *Department of Chemistry, Loyola Institute of Frontier Energy, Loyola College, Chennai, Tamil Nadu, India*

Received 11 December 2005; received in revised form 30 October 2006; accepted 11 January 2007

Abstract

Porous carbon prepared from rice husk using phosphoric acid activation through precarbonization and chemical activation has been examined for the adsorption of phenol from aqueous solutions. The method adopted could produce carbons with micro and mesoporous structure. The surface area, pore volume and pore size distribution of carbon samples activated at three different temperatures 700, 800 and 900 °C have been carried out using nitrogen adsorption isotherms at 77 K. The production yield was observed to decrease with increase in activation temperature. Adsorption behavior of phenol onto the porous carbon was studied by varying the parameters such as agitation time, phenol concentration, pH and temperature. Studies showed that the adsorption decreased with increase in pH and temperature. The sorption process was found to be exothermic in nature. The kinetic models such as pseudo first order, pseudo second order and intra particle diffusion model were fitted to identify the mechanism of adsorption process. The isotherm data were fitted to Langmuir and Freundlich models. The maximum uptake of phenol was found to be 2.35×10^{-4} mol/g at 20 °C and final pH 2.7.

Keywords: Activated carbon; Chemical activation; Surface area; Phenol adsorption

---

1. Introduction

Wastewater containing phenolic compounds presents a serious discharge problem due to their poor biodegradability, high toxicity and ecological aspects. Phenolic compounds are frequent contaminants of ground water because of their wide use in industrial sectors [1]. These are widely present in the effluents such as those generated from coal tar, plastics, leather, paint, pharmaceutical, steel, textile, timber, paper pulp, insecticides, pesticides and oil refineries [2]. In review of wastewater treatment containing phenolic compounds, it was found that adsorption by activated carbon are considered as potential treatment technique [3] and one of the best available environmental control technologies [4]. The application of carbons for adsorption from solution is probably the most important field of carbon science. The main advantages of carbon adsorption over other process are, it can remove both organic and inorganic compounds either by batch or column methods and can be regenerated for repeated use. Although porous carbons commonly known as activated carbons are extensively used for wastewater treatment, its use is often limited due to its high cost and difficult preparation methods [5,6]. This has led many workers to search for cheaper substitutes from agricultural wastes such as bagasse pith, sawdust, maize cop, coconut husk fibers, fruit kernels, nutshells, coir pith, and oil palm wastes [7]. Generally activated carbons are prepared by two different activation processes, either by physical or chemical activation. At the present time the chemical activation is preferred over physical activation for its lowered activation temperature and increased yield. Among the numerous chemical activants such as KOH, $ZnCl_2$, H_3PO_4, HCl, etc., H_3PO_4 is widely used for the process as it can be removed easily after activation of carbons by washing with hot and cold water. However phosphoric acid is preferred because it does not encounter with corrosion problem, in efficient chemical recovery and other environmental disadvantages associated with $ZnCl_2$ and other activants [8]. There has been very little or perhaps nil study using H_3PO_4 as a chemical activating agent for carbon derived from rice husk and can be obtained cheaply from the agro industries.

---

* Corresponding author. Tel.: +91 44 24911386.
E-mail addresses: jklsac14@yahoo.co.in (L.J. Kennedy), ganesansekaran@hotmail.com (G. Sekaran).

1385-8947/$ – see front matter © 2007 Elsevier B.V. All rights reserved.
doi:10.1016/j.cej.2007.01.009

In the present investigation we report the preparation of activated carbon using rice husk by phosphoric acid activation by two stage process: precarbonization and chemical activation. Activations were performed at three different temperatures 700, 800 and 900 °C in order to obtain the maximum surface area with well-developed porosity. The activated carbon obtained was employed for the adsorption of phenol from aqueous solutions. Three simplified kinetic models including pseudo first order equation, pseudo second order equation and intra particle diffusion models were used to discuss the adsorption mechanisms. The experimental data obtained were fitted to Langmuir and Freundlich models to analyze the adsorption equilibrium.

2. Experimental technique

2.1. Preparation of porous carbons

Rice husk as the precursor material obtained from the agro industry was well washed with water several times for the removal of dust and dried at 110 °C for 6 h. The dried samples were then used for the preparation of carbons.

Porous carbons were prepared in two sequential steps: precarbonization and chemical activation. In the precarbonization process the rice husk was heated to 400 °C at the rate of 10 °C/min for about 4 h under nitrogen atmosphere and cooled down to room temperature at the same rate. The resulting material is labeled as precarbonized carbon (PCC). The precarbonized carbon is then subjected to chemical activation. In chemical activation process 50 g of the precarbonized carbon was agitated with 250 g of aqueous solution containing 85% H_3PO_4 by weight. The ratio of chemical activating agent/precarbonized carbon was fixed at 4.2. The chemical activant and precarbonized carbon was homogeneously mixed at 85 °C for 4 h. After mixing the precarbonized carbon slurry was dried under vacuum at 110 °C for 24 h. The resulted samples were then activated in a vertical cylindrical furnace under nitrogen atmosphere at a flow rate of 100 ml/min to three different temperatures, 700, 800 and 900 °C at a heating rate of 5 °C/min using a programmer and maintained at the final temperature for 1 h before cooling. After cooling, the activated carbon was washed successively, several times with hot water until the pH becomes neutral and finally with cold water to remove the excess phosphorus compounds. The washed samples were dried at 110 °C to get the final product. The samples heated at activation temperatures 700, 800 and 900 °C were labeled as C700, C800 and C900.

2.2. N_2 adsorption–desorption

The N_2 adsorption–desorption isotherms of the activated carbons were measured using an automatic adsorption instrument (Quantachrome Corp. Nova-1000 gas sorption analyzer) for the determination of surface area and total pore volumes. Prior to measurement, carbon samples were degassed at 150 °C for overnight. The surface area of the activated carbons was calculated using BET equation, which is the most widely used model for determining the specific surface area (m^2/g). In addition, the *t*-plot method [9] was applied to calculate the micropore volume and external surface area (mesoporous surface area). The total pore volume was estimated as liquid volume of adsorbate adsorbed at a relative pressure of 0.99. All surface area measurements were calculated from the nitrogen adsorption isotherms by assuming the area of the nitrogen molecule to be 0.162 nm^2.

2.3. Production yield

The yield of the activated carbon is defined as the ratio of the weight of the resultant activated carbon to that of the original rice husk with both weights on dry basis [10]:

$$\text{yield}\,\% = \frac{W_2}{W_0} \times 100 \tag{1}$$

where W_0 is the original mass of the precursor on dry basis and W_2 is the mass of the carbon after activation, washing and drying.

2.4. Phenol adsorption procedure

Adsorption kinetics and equilibrium studies were conducted using batch mode adsorption technique by placing a known quantity of the adsorbent in glass bottles containing 10 ml of an aqueous solution of predetermined concentration. The activated carbon C900 that possessed comparatively highest surface area 438.9 m^2/g with particle size 600 μm was selected for the adsorption studies. The adsorbent dose was 0.15 g/10 ml solution. The solutions were agitated at 100 rpm until the equilibrium is reached at a given particular temperature, pH and concentration as agitation beyond 100 rpm had very little effect on the adsorption process. At fixed time intervals this solution was taken out and filtered and the concentration of the solute was measured spectrophotometrically by the color development method [11] as a result of the reaction of phenol with 4-aminoantipyrine. The adsorption of phenol on activated carbon from aqueous solutions were measured at four different concentrations 50, 100, 200, 300 mg/l; initial pH 2.5, 5.0, 7.5, 10.0 and at four different temperatures 20, 30, 40, and 50 °C in order to attain equilibrium and thus efficient adsorption. The mount of phenol adsorbed onto the adsorbate q_e (mmol/g) were calculated according to:

$$q_e = \frac{(C_0 - C_e)V}{W} \tag{2}$$

where V is the volume of the solution (l), C_0 the initial concentration (mmol/l), C_e the equilibrium concentration (mmol/l), and W is the weight of the adsorbent (g).

3. Results and discussion

3.1. Characterization of porous carbons

3.1.1. Nitrogen isotherms

Fig. 1 represents the nitrogen adsorption/desorption isotherms at 77 K of precarbonized carbon PCC and chemically activated carbons at temperatures 700, 800 and 900 °C being labeled as C700, C800 and C900. The isotherms of the pre-

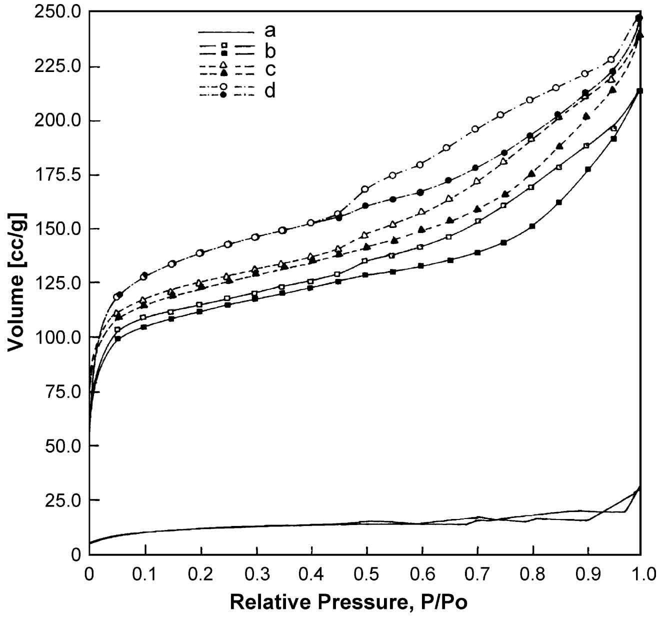

Fig. 1. Nitrogen adsorption/desorption isotherms at 77 K for (a) PCC, (b) C700, (c) C800, and (d) C900.

Table 1
Surface area and pore volume parameters of the activated carbons

S. no	Parameters	Sample code		
		C700	C800	C900
1	S_{BET} (m^2/g)	344.7	379.4	438.9
2	S_{mic} (m^2/g)	202.7	214.6	214.6
3	S_{meso} (m^2/g)	142.0	164.8	224.0
4	Micropore volume, V_{micro} (cm^3/g)	0.111	0.118	0.118
5	Mesopore volume, V_{meso} (cm^3/g)	0.223	0.255	0.268
6	Total pore volume, V_{tot} (cm^3/g)	0.335	0.373	0.387
7	$V_{\mathrm{meso}}/V_{\mathrm{tot}}$ (%)	66.78	68.41	69.33
8	Average pore diameter (Å)	38.82	39.36	35.28
9	Production yield of carbon (%)	40.66	39.19	37.69

S_{BET}, BET surface area; S_{mic}, micropore surface area; S_{meso}, mesopore surface area.

carbonized carbon (PCC) are of Type I as adsorption and the desorption branches remain nearly horizontal and parallel over a wide range of relative pressures which is the characteristic behavior of microporous material. However, for the chemically activated samples at activation temperatures 700, 800 and 900 °C the knee of the isotherms became rounded. The hysterisis effect and the slope of the plateau increased to yield Type IV isotherm with a significant increase in the nitrogen uptake through the entire pressure range indicating the presence of mesopores. This increase in uptake of nitrogen in the samples with increase in temperature is a result of the increase in porosity created in carbon matrices. Henceforth the uptake of nitrogen increases as the heat treatment temperature is increased. The carbon activated at 900 °C did exhibit the most prominent hysterisis effect which can be characterized necessarily not only by the formation of slit shaped pores but of any kind as well [9].

3.1.2. *Surface area and pore volume*

The specific surface area was calculated using the BET model. Mesopore surface area was calculated by the *t*-plot method. The precarbonized carbon had very low surface area 55 m^2/g. The BET surface area increased considerably after impregnation and activation at higher temperatures. The nitrogen BET surface area increased with activation temperature as shown in Table 1. The increase in surface area can be attributed to the release of certain volatile components from the work generated by acid treatment on the precursor material containing the organic and inorganic matter over the temperature 700–900 °C. Consequently pores of different dimensions are produced. The mesoporous surface area increases steeply especially for the samples C800 and C900. The micropore surface area was obtained by subtracting mesopores surface area from the corresponding BET surface area. There is only a narrow increase in the micropore surface area for the sample C800 with respect to C700. But with reference to the sample C900 the micropore surface area becomes almost constant with a significant increase in the mesopores. These results suggest that at higher activation temperatures new pores created were enlarged or widened to fall in the mesoporic range.

Heat treatment temperature has a pronounced effect on pore volume profile. Total pore volumes were estimated from nitrogen adsorption at a relative pressure of 0.99. Micropore volumes were obtained by *t*-plot method. The mesopore volume was calculated by subtracting micropore volume from the total pore volume. The increase in total pore volume is only with in a small range. The percentage of micropore volume was observed to be a near constant with rise in temperature. There was a considerable linear increase in mesopore volume from 0.223 to 0.268 cm^3/g at heat treatment temperature 700 and 900 °C, respectively. The increase in mesopore volume can be attributed to simultaneous pore opening and pore widening by the activating agents, but at higher temperature 900 °C the pore widening effect dominates the pore opening effect [12]. The mesoporosity (percentage of mesopores to total pore volume $V_{\mathrm{meso}}/V_{\mathrm{tot}}$) of the carbon samples were in the range between 66.78 and 69.33% corresponding to C700 and C900, respectively as shown in Table 1. Table 1 also reveals that the mesopore volume of C700, C800 and C900 samples were respectively 0.223, 0.255 and 0.268 cm^3/g. The data suggests that the increase in temperature created new pores that were widened immediately to the mesoporic range. This result is in good agreement with the results of the total surface area measurement, which increased with increase in temperature. These results suggest that the heat treatment at 900 °C can be considered as the optimum temperature for the production of mesoporous activated carbons.

3.1.3. *Pore size and pore distribution*

Fig. 2 shows the pore size distribution of activated carbon samples. The average pore size distribution is dependent mainly on the concentration of chemical impregnation and heat treatment temperature. The average pore diameter of 38.8 Å was obtained at activation temperature 700 °C and later on increased with activation temperature up to 800 °C but reversed at further higher temperature. The activated carbon obtained at 700 °C characterized by an average pore diameter of 38.8 Å is seen to

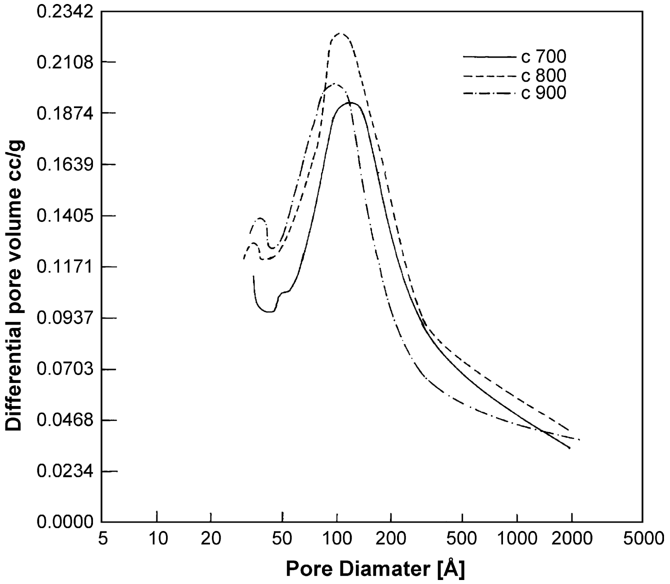

Fig. 2. Pore size distributions for activated carbon C700, C800 and C900 carbon samples.

have a marginal increase in pore diameter of 39.36 Å at 800 °C. The narrow increase in pore diameter suggest that at 800 °C, certain unorganized carbons or residual tar materials were expelled by opening of closed pores [13] and existing pores, widened into larger pores of small magnitude through gasification of carbons in the pore walls having labile carbon structure [10]. The decrease in the pore diameter of C900 is due to the suppression of the pore widening of stable carbon structures [14] formed during precarbonization process and coalescence of pores in the carbon matrices.

3.1.4. Production yield

The precarbonized carbon yield was 53%. However, after H_3PO_4 impregnation, activation and washing the carbon yield corresponding to C700, C800 and C900 were in the range 41–38% as presented in the Table 1. The difference in the carbon yield between the precarbonization and activation stages was due to further removal of strongly held volatiles through opening of the closed pores at high temperatures. A decrease in the yield of the carbon with increase in activation temperature can also be accounted by the gasification of carbons during the process [15]. The carbon C900 that had maximum surface area as shown in Table 1 and its characteristics shown in Table 2 was selected for phenol adsorption studies.

Table 2
Characteristics of C900 porous carbon

S. no	Parameter	Value
1	Carbon (%)	37.96
2	Hydrogen (%)	2.4 6
3	Nitrogen (%)	0.50
4	Others (%)	59.08
5	Bulk density (g/cm^3)	0.56
6	pH_{PZC}	7.1

3.2. Phenol adsorption

3.2.1. Effect of time

The effect of time for adsorption process was carried out to determine the equilibrium point. The study was carried out at four different temperatures, pH and concentration. It was found for all the set of experiments, the adsorption was rapid up to 15 min and latter on became slow, and finally the systems reached equilibrium around 75 min. Henceforth the maximum time of adsorption was restricted up to 75 min. The amount adsorbed (mmol/g) increased with increase in agitation time until equilibrium and the curves for phenol adsorption with respect to time were single smooth and continuous leading to saturation.

3.2.2. Effect of pH

One of the critical parameter in the treatment of phenol by the sorption medium is pH. pH primarily affects the degree of ionization of the phenolic sorbate. The uptake of phenol by the activated carbon varies with pH as shown in Fig. 3. The adsorption decreases with increase in pH. The point of zero charge of the carbon was found to be 7.1. The pH was measured before and after adsorption process and it has been found that the final pH were 2.7, 5.2, 7.4 and 9.4. Thus the optimum pH for the removal of phenol by the mesoporous carbon was chosen as pH 2.5 ± 2 as it showed maximum uptake of phenol than the other pHs. When pH exceeded 7.5 there was a fall in the uptake of phenol. This can be attributed to the dependency of phenol ionization on the pH value and point of zero charge (pH_{PZC}) for mesoporous carbon. As the pH is increased the percentage of the unionized species of the compound decreases and of the ionized species increases. At pH 2.5 (final pH $2.7 < pH_{PZC}$), the carbon surface is positively charged and as there is no electrostatic repulsion between the unionized phenol species and the positively charged surface and thus adsorption is higher. But at pH 10 (final pH $9.4 > pH_{PZC}$) the carbon surface is negatively charged resulting in reduced adsorption due to the repulsive force between the phenolate ion and negative charge of the carbon surface. This occurs based on the relationship [16]:

$$P_0 = \frac{P_T}{[1 + 10^{pK_a - pH}]} \tag{3}$$

where P_0 is the concentration of unionized phenol species, P_T the total concentration of phenol taken, pH the final pH (equilib-

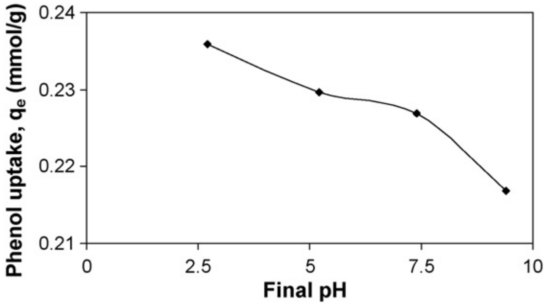

Fig. 3. Effect of pH on the uptake of phenol onto activated carbon (concentration 3.187 mmol/l, temperature 20 °C).

rium pH) after adsorption and pK_a is 10. Despite the electrostatic repulsion at pH 10 (final pH 9.4), a significant adsorption takes place indicating that chemisorption might be involved in the process [17]. Similar results were reported in the adsorption of phenol and substituted phenols [18].

3.2.3. *Effect of concentration and temperature*

The sorption capacity of the activated carbon increased with increase in phenol concentration. When the initial phenol concentration was increased from 0.531 to 3.187 mmol/l, the loading capacity increased from 3.89×10^{-5} to 2.35×10^{-4} mol/g of dried carbon. It is evident that most of the adsorption sites are filled up in the very early time period of ∼15 min at all the concentrations. Initially the number of adsorption sites available is higher and the driving force for the mass transfer is greater. Therefore the adsorbate reaches the adsorption site with ease. With time, number of active sites becomes less and the adsorbent becomes crowded inside the particles, thus impeding the movement of the adsorbate. This can be accounted for the decrease in adsorption rate after 15 min. Thus, the initial concentration provides an important driving force to overcome all mass transfer resistances of phenol between the aqueous and solid phases [19]. Hence, higher concentration of phenol enhances the sorption process.

The plot of adsorption capacity as a function of temperature is shown in Fig. 4. The equilibrium uptake of phenol molecules onto the activated carbon decreased with increase in temperature from 20 to 50 °C indicating less chemical interaction between the sorbate and the surface functionalities of the active carbons. Phenol adsorption was exothermic and thus the extent of adsorption decreased with increase in temperature.

3.2.4. *Kinetic modeling*

In order to investigate the adsorption process of phenol onto mesoporous carbon, the frequently used kinetic models such as the linearised form of pseudo first order, pseudo second order and intra particle diffusion models given in Eqs. (4)–(6), respectively were used to determine the mechanism of adsorption process. The equations are represented as [20–23]:

$$\ln(q_e - q_t) = \ln q_e - k_1 t \tag{4}$$

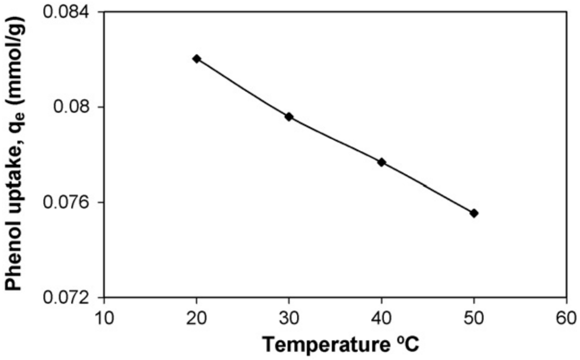

Fig. 4. Uptake of phenol onto activated carbon at different temperatures (concentration 1.06 mmol/l, final pH 7.4).

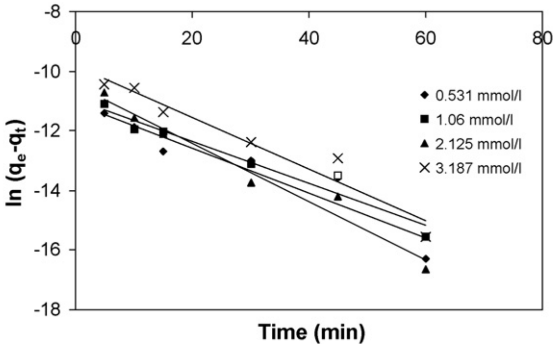

Fig. 5. Plot of first order kinetic model at different concentrations (temperature 20 °C, final pH 2.7).

$$\frac{t}{q_t} = \frac{1}{k_2 q_e^2} + \frac{1}{q_e} t \tag{5}$$

$$q_t = k_d \sqrt{t} \tag{6}$$

where q_e and q_t are the amount of phenol adsorbed (mmol/g) at equilibrium and at time (min), k_1 is the first order equilibrium rate constant (min^{-1}), k_2 the pseudo second order rate constant and k_d is the intraparticle diffusion rate constant (mol/gmin$^{-1/2}$).

The pseudo first order, second order and intraparticle diffusion rate constants were evaluated from the linear plots of $\ln(q_e - q_t)$ versus t, t/q_t versus t and q_t versus $\sqrt{t}$, respectively and are shown in Figs. 5–7. The correlation coefficient (R^2) calculated from these plots was used to evaluate the applicabil-

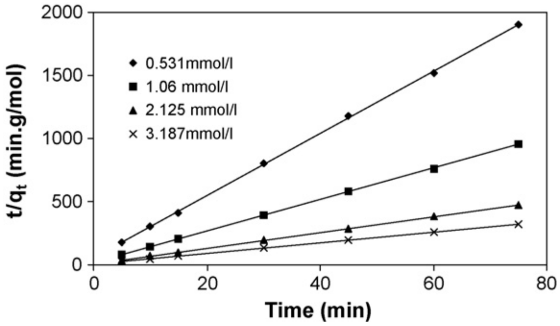

Fig. 6. Plot of second order kinetic model at different concentrations (temperature 20 °C, final pH 2.7).

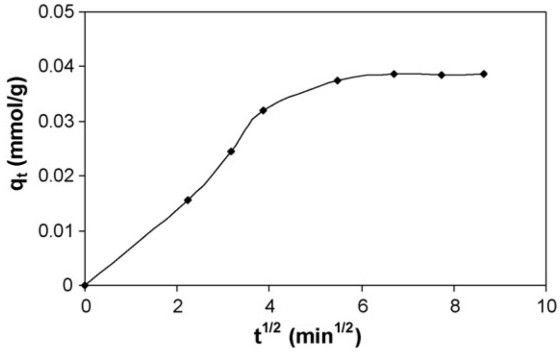

Fig. 7. Plot of Weber and Morris equation for phenol adsorption (concentration 0.531 mmol/l, temperature 50 °C, final pH 2.7).

Table 3
Comparison of the first, second order and diffusion rate constants values for phenol adsorption (final pH 2.7, concentration 3.187 mmol/l)

Temperature (°C)	% removal	Amount adsorbed q_e, (mmol/g)	First order kinetic model		Second order kinetic model		Diffusion model		Diffusivity, $D \times 10^{-11}$ (m^2/s)
			k_1 (min^{-1})	R^2	$k_2 \times 10^3$ (g/(mol min))	R^2	k_d (mg g^{-1} min$^{-1/2}$)	δ (mg/g)	
20	94.39	0.233	0.086	0.945	5.078	0.999	0.198	20.90	6.64
30	93.33	0.231	0.049	0.921	4.264	1.000	0.166	19.16	6.42
40	91.16	0.225	0.007	0.830	3.929	1.000	0.125	18.10	6.15
50	90.00	0.222	0.075	0.957	3.562	0.999	0.083	17.56	6.00

ity of these models. The analysis of the correlation coefficients (R^2) shown in Table 3 suggests that the experimental data fit the pseudo second order model with R^2 values greater than 0.999 than that of the pseudo first order model with R^2 values ranging between 0.830 and 0.957.

The intraparticle diffusion was also involved in the adsorption of phenol onto activated carbon and is shown in Fig. 7. Previous studies showed that such plots may present a multilinerarity, which indicates that two or more steps occur. The first sharper portion is the external surface adsorption or instantaneous adsorption stage. The second portion is the gradual adsorption stage, where the intraparticle diffusion is rate limited. The third portion is final equilibrium stage, where the intraparticle diffusion starts to slow down due to extremely low soluble concentration in the solution. The diffusion model plot shown in Fig. 7 suggests two-stage adsorption process, surface adsorption and intraparticle diffusion. The first linear portion of the plot indicates boundary layer effect, i.e. surface adsorption while the second linear portion is due to the intraparticle/pore diffusion within the pores of the carbon. The slope of the second linear portion of the plot has been defined as a rate parameter (k_d), which characterizes the rate of adsorption in the region where pore diffusion is rate limiting. The intercept of the plot (δ) on the other hand signifies the extent of boundary layer effect [24]. The intercept of the plot and the slope signifying the rate parameter are listed in the Table 3. The two different regions of rates of uptake observed in the study indicate that the rate of uptake is initially slightly faster and then slows down. It is likely that initially the adsorbate is transported to the macropore and mesopore and then it is slowly diffused into micropores [25]. Thus all these suggest that in the adsorption of phenol over the carbon was controlled by external mass transfer followed by intra particle diffusion mass transfer.

The pore diffusion coefficient, D for the uptake of phenol by the mesoporous carbon have been calculated using the Eq. (7), assuming the spherical shape geometry for the adsorbent particles [26]:

$$D = \frac{0.03 r_0^2}{t_{1/2}} \tag{7}$$

where r_0 is the diameter of the particle, $t_{1/2}$ the time for half adsorption and D is the pore diffusion constant (m^2/s). The values of the pore diffusion constants were found to be of the order of 10^{-11} m^2/s for the studied range of pH, concentration and temperatures. The highest value of 6.64×10^{-11} m^2/s was obtained at pH 2.5, concentration 3.187 mmol and temperature 20 °C as shown in the Table 3.

3.2.5. Adsorption isotherms

Langmuir and Freundlich models [27–29] are the most frequently employed models among the several available models to describe the experimental data of adsorption isotherms. The Langmuir equation is applicable to homogeneous sorption where the sorption of each sorbate molecule on to the surface has equal sorption activation energy and is represented by the expression:

$$q_e = \frac{K_L C_e}{1 + a_L C_e} \tag{8}$$

where q_e is the solid phase sorbate concentration at equilibrium (mmol/g), K_L is the Langmuir isotherm constant (l/g), a_L is the Langmuir isotherm constant (l/mmol).

The linearised form of Langmuir equation is given as

$$\frac{C_e}{q_e} = \frac{1}{K_L} + \frac{a_L}{K_L} C_e \tag{9}$$

The sorption data were analyzed according to the linear form of equation mentioned above. The constants were evaluated from the slope a_L/K_L and intercept $1/K_L$ of the linear plot of C_e/q_e versus C_e, where K_L/a_L gives the theoretical monolayer saturation capacity Q_0. The isotherms at all the range of studied pH and temperatures were not found to be linear almost over the whole range of concentrations as evidenced from the values of correlation coefficients (R^2) obtained in the range 0.734–0.992. This implies that the adsorption equilibrium data do not exactly fit the Langmuir model of adsorption. The isotherm constants K_L, a_L and the equilibrium monolayer capacities Q_0 are represented in the Table 4.

The most important multisite adsorption isotherm for heterogeneous surfaces is the Freundlich adsorption isotherm that is characterized by the heterogeneity factor $1/n$ and is represented by the equation:

$$q_e = K_F C_e^{1/n} \tag{10}$$

where q_e is the solid phase concentration in equilibrium (mmol/g), C_e is the liquid phase sorbent concentration at equilibrium (mmol/l), K_F is the Freundlich constant (l/g) and $1/n$ is the heterogeneity factor.

The linearised form of the Freundlich equation is:

$$\ln q_e = \ln K_F + \frac{1}{n} \ln C_e \tag{11}$$

Table 4
Langmuir sorption isotherm constants for the adsorption of phenol on to activated carbon

Final pH	Temperature															
	20 °C				30 °C				40 °C				50 °C			
	K_L (l/g)	$a_L \times 10^3$ (l/mol)	Q_0 (mmol/g)	R^2	K_L (l/g)	$a_L \times 10^3$ (l/mol)	Q_0 (mol/g)	R^2	K_L (l/g)	$a_L \times 10^3$ (l/mol)	Q_0 (mol/g)	R^2	K_L (l/g)	$a_L \times 10^3$ (l/mol)	Q_0 (mol/g)	R^2
2.7	2.06	3.13	0.661	0.941	1.832	2.98	0.614	0.925	1.411	2.65	0.531	0.992	1.194	2.35	0.507	0.937
5.2	1.32	2.07	0.635	0.857	0.979	1.70	0.575	0.750	0.889	1.69	0.526	0.763	0.767	1.58	0.485	0.920
7.4	1.13	1.91	0.591	0.746	0.856	1.57	0.543	0.664	0.696	1.41	0.493	0.972	0.601	1.30	0.461	0.973
9.4	0.82	1.57	0.525	0.824	0.616	1.22	0.506	0.734	0.574	1.20	0.475	0.823	0.339	1.03	0.298	0.903

Table 5
Freundlich sorption isotherm constants for the adsorption of phenol on to activated carbon

Final pH	Temperature											
	20 °C			30 °C			40 °C			50 °C		
	K_F [(mol/g)(mol/l)^n]	$1/n$	R^2	K_F [(mol/g)(mol/l)^n]	$1/n$	R^2	K_F [(mol/g)(mol/l)^n]	$1/n$	R^2	K_F [(mol/g)(mol/l)^n]	$1/n$	R^2
2.7	0.329	0.833	0.989	0.286	0.830	0.983	0.153	0.790	0.993	0.112	0.772	0.997
5.2	0.206	0.824	0.989	0.139	0.809	0.982	0.105	0.787	0.988	0.085	0.780	0.987
7.4	0.159	0.811	0.984	0.107	0.799	0.985	0.079	0.780	0.999	0.064	0.772	0.997
9.4	0.103	0.793	0.991	0.082	0.791	0.975	0.069	0.782	0.984	0.051	0.689	0.986

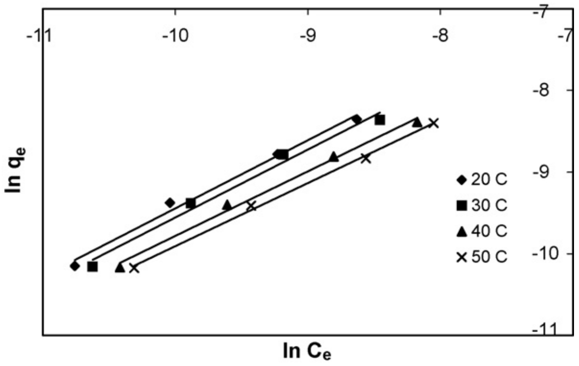

Fig. 8. Freundlich isotherm model at different temperatures at final pH 2.7.

The plot of $\ln q_e$ versus $\ln C_e$ enables the constants K_F and exponent $1/n$ to be determined as shown in Fig. 8. The Freundlich isotherm describes reversible adsorption and is not restricted to the formation of monolayer. Examination of the data derived from the linearised Freundlich equations provides a good adsorption for over the range of pH, temperature and the concentration range studied as evidenced from the highest coefficient of correlation R^2 between 0.975 and 0.999. Table 5 shows the Freundlich sorption isotherm constants K_F and $1/n$. The K_F values were observed to decrease with increase in pH and temperature due to the decrease in the adsorption capacity. The highest K_F values were found as 0.329 at the condition of final pH 2.5 and temperature 20 °C. Similarly the lowest value of 0.051 of K_F was obtained at pH 10 and temperature 50 °C. The experimental data as observed from Table 5 indicates that '$1/n$' is less than unity, indicating that phenol molecules are favorably adsorbed by the dried activated carbon at all temperatures.

4. Conclusion

The chemical activation at 900 °C was found to be the optimum within the experimental range of temperatures tested for the preparation of better carbon from rice husk by the two-stage process. The use of phosphoric acid had the effect of producing considerable quantities of micropores and mesopores and the inclusion process prior to chemical activation makes the process simpler and cheaper. The carbon was found to be a suitable adsorbent. The carbon sample C900 that possessed maximum total surface area of 438.9 m^2/g and mesopore surface area 224 m^2/g was employed for phenol adsorption. The optimum condition for adsorption of phenol was at final pH 2.7 and temperature 20 °C with maximum uptake of 2.35×10^{-4} mol/g. The kinetics of phenol adsorption well followed the pseudo second order rate equation. Among the models of Langmuir and Freundlich, the best-fit equilibrium model for the sorption of phenol onto activated carbon, C900 that could represent the isotherm data was the Freundlich equation. On the basis of the data, it can be concluded that abundant availability of rice husk of little utility can be carbonized and can behave as a suitable adsorbent. The investigations would be are quite useful in developing an appropriate technology for wastewater treatment.

Acknowledgement

The authors highly thank the council of scientific and industrial research (CSIR), India for providing financial assistance to the first author during the course of the work.

References

[1] E. Sabio, M.L.G. Martin, A. Ramiro, J.F. Gonzalez, J.M. Bruque, L.L. Broncano, J.M.J. Encinar, Influence of regeneration temperature on the phenols adsorption on activated carbon, Colloid Interface Sci. 242 (2001) 31.
[2] P. Podkoscielny, A. Dabrowski, O.V. Marijuk, Heterogeneity of activated carbons in adsorption of phenol aqueous solutions, Appl. Surf. Sci. 205 (2003) 297.
[3] C. Carlos Moreno, Adsorption of organic molecules from aqueous solutions on carbon materials, Carbon 42 (2004) 83.
[4] S.H. Lin, Y.H.J. Cheng, Adsorption of BTEX from aqueous solutions by macro reticular resins, J. Hazard. Mater. 70 (1999) 21.
[5] J. Ruey-Shin, W. Feng-Chin, Ru-Ling, Characterization and use of activated carbons prepared from bagasses for liquid-phase adsorption, Colloids Surf. A: Physicochem. Eng. Aspects 201 (2002) 191.
[6] B.C. Pan, Y. Xiong, Q. Su, A.M. Li, J.L. Chen, Q.Z. Zhang, Role of amination of a polymeric adsorbent on phenol adsorption from aqueous solution, Chemosphere 51 (2003) 953.
[7] L. John Kennedy, J.J. Vijaya, G. Sekaran, Effect of two stage process on the preparation and characterization of porous carbon composite from rice husk by phosphoric acid activation, Ind. Eng. Chem. Res. 43 (2004) 1832.
[8] T. Heisheng, Y. Tien-Sheng, H. Li-Yeh, Prepration of activated carbon from bituminous coal with phosphoric acid activation, Carbon 36 (1998) 1387.
[9] S.J. Gregg, K.S.W. Sing, Adsorption, Surface Area and Porosity, Academic Press, London, 1982, 100.
[10] D. Yulu, W.P. Walawender, L.T. Fan, Activated carbons prepared from phosphoric acid activation of grain sorghum, Bioresour. Technol. 81 (2002) 45.
[11] K. Mohanty, D. Das, M.N. Biswas, Adsorption of phenol from aqueous solutions using activate carbons prepared from Tectona grandis sawdust by $ZnCl_2$ activation, Chem. Eng. J. 115 (2005) 121.
[12] H.Y. Chang, Y.H. Park, C.R. Park, Effect of precarbonization on porosity development of activated carbons from rice straw, Carbon 39 (2001) 559.
[13] O. Gyu Hwan, C.R. Park, Preparation and characterization of rice straw based porous carbons with high adsorption capacity, Fuel 81 (2002) 327.
[14] H. Marsh, K. Kuo, Kinetics and catalysis of carbon gasification, in: H. Marsh (Ed.), Introduction to Carbon Science, Butterworth, London, 1989, p. 107.
[15] T. Wigman, Industrial aspects of production and use of activated carbons, Carbon 27 (1989) 13.
[16] F.A. Banat, B. Al-Basher, S. Al-Asheh, O. Hayajneh, Adsorption of phenol by bentonite, Environ. Pollution 107 (2000) 391.
[17] C. Namasivayam, D. Kavitha, Adsorptive removal of 2-chlorophenol by low cost coir pith carbon, J. Hazard. Mater. 98 (2003) 257.
[18] C. Namasivayam, D. Kavitha, Removal of phenol and chlorophenols from water by coir pith, J. Environ. Sci., Eng. 46 (2003) 217.
[19] D.M. Nevskaia, A. Santianes, V. Munoz, A. Guerrero-Ruiz, Interaction of aqueous solutions of phenol with commercial activated carbons: an adsorption and kinetic study, Carbon 37 (1999) 1065.
[20] Z. Aksu, Y.A. Julide, Comparative adsorption/biosorption study of monochlorinated phenols onto various sorbents, Waste Manage. 2 (2000) 695.
[21] F.A. Banat, S. Al-Asheh, L. Al-Makhadmeh, Utilization of raw and activated date pits for the removal of phenol from aqueous solutions, Chem. Eng. Technol. 27 (2004) 80.
[22] R.S. Juang, C.W. Feng, R.L. Tseng, Mechanism of adsorption of dyes and phenols from water using activated carbons prepared from plum kernels, J. Colloid Interface Sci. 227 (2000) 437.

[23] W.J. Weber, J.C. Morris, Proceedings of the International Conference on Water Pol. Symposium, vol. 2, Pergmon Press, Oxford, 1962, p. 231.
[24] S. Mitali, A. Pradeep Kumar, B. Bhasker, Modeling the adsorption kinetics of some priority organic pollutants in water from diffusion and activated energy parameters, J. Colloid Interface Sci. 206 (2003) 28.
[25] K. Arinjay, K. Shashi, K. Surendra, Adsorption of resorcinol and catechol on granular activated carbon: equilibrium and kinetics, Carbon 41 (2003) 3015.
[26] M. Ahmaruzzaman, D.K. Sharma, Adsorption of phenols from wastewater, J. Colloid Interface Sci. 287 (2005) 14.
[27] R.L. Tseng, F.C. Wu, R.S. Juang, Liquid phase adsorption of dyes and phenols using pine wood based activated carbon, Carbon 41 (2003) 487.
[28] I. Langmuir, The adsorption of gases on plane surfaces of glass, mica and platinum, J. Am. Chem. Soc. 40 (1918) 1361.
[29] H.M.F. Freundlich, Over the adsorption in solution, J. Phys. Chem. 57 (1906) 385.